
Research Article

Theme: Fishing for the Hidden Proteome in Health and Disease: Focus on Drug Abuse
Guest Editors: Rao S. Rapaka, Lloyd D. Fricker, and Jonathan V. Sweedler

Investigation of the Ovarian and Prostate Cancer Peptidome for Candidate Early Detection Markers Using a Novel Nanoparticle Biomarker Capture Technology

Claudia Fredolini,^{1,2,7} Francesco Meani,^{3,7} Alessandra Luchini,⁷ Weidong Zhou,⁷ Paul Russo,⁷ Mark Ross,⁷ Alexis Patanarut,^{4,7} Davide Tamburro,^{5,7} Guido Gambara,⁷ David Ornstein,⁶ Franco Odicino,³ Monica Ragnoli,³ Antonella Ravaggi,³ Francesco Novelli,² Devis Collura,¹ Leonardo D'Urso,¹ Giovanni Muto,¹ Claudio Belluco,⁸ Sergio Pecorelli,³ Lance Liotta,⁷ and Emanuel F. Petricoin III^{7,9}

Received 4 March 2010; accepted 1 June 2010; published online 12 June 2010

Abstract. Current efforts to identify protein biomarkers of disease use mainly mass spectrometry (MS) to analyze tissue and blood specimens. The low-molecular-weight “peptidome” is an attractive information archive because of the facile nature by which the low-molecular-weight information freely crosses the endothelial cell barrier of the vasculature, which provides opportunity to measure disease microenvironment-associated protein analytes secreted or shed into the extracellular interstitium and from there into the circulation. However, identifying useful protein biomarkers (peptidomic or not) which could be useful to detect early detection/monitoring of disease, toxicity, doping, or drug abuse has been severely hampered because even the most sophisticated, high-resolution MS technologies have lower sensitivities than those of the immunoassays technologies now routinely used in clinical practice. Identification of novel low abundance biomarkers that are indicative of early-stage events that likely exist in the sub-nanogram per milliliter concentration range of known markers, such as prostate-specific antigen, cannot be readily detected by current MS technologies. We have developed a new nanoparticle technology that can, in one step, capture, concentrate, and separate the peptidome from high-abundance blood proteins. Herein, we describe an initial pilot study whereby the peptidome content of ovarian and prostate cancer patients is investigated with this method. Differentially abundant candidate peptidome biomarkers that appear to be specific for early-stage ovarian and prostate cancer have been identified and reveal the potential utility for this new methodology

KEY WORDS: Peptidome; Cancer; Biomarker; Nanoparticle; Mass spectrometry.

Claudia Fredolini and Francesco Meani equally contributed to this work.

¹ Department of Urology, S. Giovanni Bosco Hospital, Turin, Italy.

² Department of Medicine and Experimental Oncology, University of Turin, Turin, Italy.

³ Gynecology and Obstetrics Department, University of Brescia, Brescia, Italy.

⁴ Chemistry and Biochemistry Department, George Mason University, Manassas, Virginia, USA.

⁵ Department of Hematology, Oncology and Molecular Medicine, Istituto Superiore di Sanità, Rome, Italy.

⁶ Department of Urology, University of California at Irvine, Irvine, California, USA.

⁷ Center for the Applied Proteomics and Molecular Medicine, George Mason University, 10900 University Blvd, Room 181A Discovery Hall, Manassas, Virginia 20110, USA.

⁸ Department of Experimental Oncology 2, CRO-IRCSS, National Cancer Institute, Aviano, Italy.

⁹ To whom correspondence should be addressed. (e-mail: epetrico@gmu.edu)

INTRODUCTION

Prostate and ovarian cancers pose a great health burden on world population principally due to the very high incidence and variability in the clinical course of the former and overall poor prognosis of the latter. Prostate cancer (CaP) is an age-related tumor as it accounts for about 25% of all the newly diagnosed cancers in American men and caused more than 28,000 deaths in 2008. As the population ages, the number of new cases per year is expected to increase by >60% and reach 300,000 by 2015 (1). This high incidence, coupled with the clinical course variability of the disease, makes CaP a particularly appropriate candidate for prevention and early intervention strategies.

Since the FDA approval and introduction into the clinic in the mid-1980s, the prostate-specific antigen (PSA) levels combined with digital rectal examination are the standard screening tests for the early detection of prostate cancer (2). The European Randomized Study of Screening for Prostate Cancer, initiated in the early 1990s and ended in 2006 to evaluate the effect of

screening with PSA, concluded that PSA-based screening reduced the rate of death from prostate cancer by 20%, but is associated with a high risk of overdiagnosis (3). Actually, PSA is secreted from benign as well as cancerous cells of the prostate, and it has been demonstrated to be mostly a marker of prostate volume than of malignant conditions (4). An increase in prostate volume, naturally growing with age, can occur for benign as well as for pathologic conditions, and thus, serum PSA values correlate closely with both benign prostatic hyperplasia and CaP (4). Moreover, while it appears that some levels of CaP biopsies are carried out without actual clinical necessity (with the associated economic and social consequences), 15% of patients with levels of PSA lower than the recognized 4 ng/ml disease diagnosis threshold have cancer, with some of these being very lethal aggressive forms (5). Indeed, PSA is unable to predict with certainty the biological aggressiveness of the disease, so prostate cancer screening results in the detection of disease that in many patients is not clinically significant.

Ovarian cancer (OC), according to the late onset of symptoms and the subsequent poor prognosis by the time of diagnosis, has come to be known by the haunting definition of “the silent killer.” OC is the fourth most frequent cause of cancer death and the most lethal of all gynecologic tumors in women from North America and northern and western Europe. Each year, approximately 20,000 American women are diagnosed with ovarian cancer and about 15,000 women die from the disease. The median age at diagnosis is 63. In 2009, the National Cancer Institute estimated that 21,650 women in the USA would be diagnosed with ovarian cancer and 15,520 women would die from the disease (6). Despite its incidence being ten times lower than breast cancer, it is threefold more lethal and is usually not diagnosed until its advanced stages. The prognosis for survival from ovarian cancer largely depends on the extent of disease at diagnosis: while the overall 5-year relative survival rate for all women with ovarian cancer is 46%, this rate improves greatly to 93% if the cancer is diagnosed at an early stage before it has spread beyond the ovaries (7,8). Accordingly, detection of early stage disease offers an opportunity to reduce mortality. Unfortunately, to date, no screening protocol for ovarian cancer has been shown to achieve this aim, and only 19% of ovarian cancer cases are diagnosed at local stage (9,10)

Despite advances in molecular biology, surgery, and chemotherapy, survival rates have changed very little in the last three decades. The glycoprotein CA-125 is the most thoroughly investigated biomarker for ovarian cancer screening and is currently the only marker used in combination with transvaginal ultrasound to detect a significant proportion of ovarian cancer (8,11–13). The serum CA 125 assay has been evaluated for ovarian cancer screening as a tool to differentiate benign from malignant ovarian masses and as an indicator of tumor status during and after chemotherapy. Unfortunately, CA-125 has not been found to be sufficiently specific or sensitive for screening the general population. It is believed that up to 20% of ovarian cancers do not express CA-125, suggesting a maximum theoretical sensitivity of 80% for this marker, and for early-stage disease, this theoretical sensitivity is likely to be lower (7,8,13).

Consequently, ovarian and prostate cancers share unsolved diagnostic and therapeutic dilemmas, underpinning the need for new reliable biomarkers for early detection and better prognostic classification. Blood-borne biomarkers cur-

rently available for these two cancers do not fulfill the requirements for implementing reliable and acceptable screening tests on the general population currently performing a tissue biopsy represents the only definitive way to achieve diagnosis. Thus, the search for new, highly sensitive and specific markers, and combinations or signatures of multiple markers, has been intensive. The circulatory proteome has become one of the most promising molecular archives for the discovery of biomarkers of human diseases (14–17). Even as some investigators have turned their attention to urine and abdominal fluid as a source of molecular diagnostic information for prostate and ovarian cancers, among all physiological fluids, human plasma and serum have become the most intensively investigated biological samples. Blood, since it flows through the entire body every second, can be considered to most accurately reflect ongoing physiology and represents a protein-rich information reservoir, containing the traces of what has been encountered during constant perfusion of tissues (18).

Due to the ability of the technique to investigate and profile the complex proteomes of biological specimens in an unbiased fashion, mass spectrometry (MS)-based proteomic technologies are currently at the forefront for the discovery of blood-borne biomarkers. Of special recent interest in biomarker discovery efforts, the peptidome, or low-molecular-weight (LMW) proteome, may likely contain many of the most clinically important undiscovered markers since this repository contains analytes that are able to passively diffuse through the endothelial cell barrier of the vasculature, a barrier that effectively prevents the passive perfusion of molecules above 60 kDa. The *peptidome* contains protein fragments and small protein molecules generated within the tissue microenvironment that could reflect early-stage pathophysiological changes (19).

However, despite the recent technological advances in mass spectrometry and sample fractionation methods, analytical and physiological barriers hinder the deep exploration of circulatory peptidome and biological marker discovery. Firstly, most biomarkers that will have any clinical impact on early cancer detection will be found in very low abundances, with concentrations likely in the sub-nanogram per milliliter range, well below the detection limits of even the most sophisticated MS instrumentation. A second major problem is the apparently insurmountable abundance of resident proteins such as albumin and immunoglobulins, which hinder the MS identification of new candidate biomarkers, that may be one billion or more times less abundant than these endogenous proteins. Moreover, most of the time, low abundance biomarkers are non-covalently and endogenously associated with resident proteins that account for >95% of circulating proteins, confounding the isolation of rare LMW biomarkers (19–25). As a consequence, many researchers endeavor in the extremely complicated and time-consuming task to enrich the biospecimen for targeted analytes, attempting to avoid loss of the LMW fraction bound to high-molecular-weight proteins.

To that end, herein we present a novel method for body fluid-based biomarker discovery in which a novel nanoparticle-based biomarker capture technology is applied to amplify, fractionate, and enrich the LMW peptidome archive providing a powerful pre-analytical (MS) concentration and fractionation method for mass spectrometry-based biomarker discovery. We have developed these core-shell hydrogel nanoparticles to perform, in solution and in one step, the rapid (within 30 min)

Table I. Clinical Features of Prostate Cancer Patients Included in the Study

Age	Pre-surgical PSA (ng/ml)	c-stage	Gleason score biopsy	Bx	Lymph node status
48	8.1	T1c	3+3=6	Left	No
63	5.3	T2b	3+4=7	Bilateral	Yes
66	4.9	T1c	3+3=6	Bilateral	Yes
67	6.3	T1c	3+3=6	Left	No
69	7	T1c	3+4=7	Left	No
62	5.7	T1c	4+4=8	Right	Yes
72	8.6	T1c	3+3=6	Right	No
67	3.1	T1c	3+3=6	Right	No
70	5.1	T1c	3+3=6	Right	No
68	8.3	T1c	3+3=6	Right	No
55	7.3	T1c	3+4=7	Bilateral	Yes
70	10.7	T2a	3+4=7	Bilateral	Yes
55	16.3	T1c	3+3=6	Right	Yes
63	5.7	T1c	3+3=6	Right	No
78	4.1	T1c	3+3=6	Right	No

complete sequestration of the peptidome simultaneously performing size sieving enrichments and dramatic concentration of the LMW analytes (26,28). The bait within the particles, comprising a high-affinity dye molecule, competes with carrier proteins such as albumin for the binding of LMW cationic proteins and peptides that are thus trapped in the particle. The shell acts as a sieve, excluding high molecular weight, high abundance proteins. Feasibility of this workflow is presented whereby LMW candidate biomarkers have been identified using well-controlled study sets of serum samples from patients with and without CaP or OC that are processed through nanoparticle enrichment followed by high-resolution MS to illustrate the potential of this new workflow.

MATERIALS AND METHODS

Synthesis and Characterization of Hydrogel NIPAm/AAc Core-Shell Particles

Particles were synthesized as previously described (26–28) using NIPAm (Sigma-Aldrich) and BIS (Sigma-Aldrich) by precipitation polymerization. Acrylic acid (AAc; Sigma-Aldrich) was incorporated into NIPAm particle to provide a charge-based affinity moiety bait for affinity capture of peptides and small molecules

Sera Sample Collection and Storage

Urologic Patients

A unique study set of 30 patient-matched serum samples were obtained from 15 patients suffering from prostate cancer under full IRB approval and patient consent. The pretreatment serum was collected before radical prostatectomy and the post-surgery samples obtained 6 weeks to 3 months afterward. Patient epidemiologic and clinical information is shown in Table I.

Gynecological Patients

A study set of serum samples from 20 early-stage epithelial ovarian cancer patients and 20 patients affected by

benign gynecologic disease requiring surgical intervention (controls) was collected at the Department of Obstetrics and Gynaecology, University of Brescia, Italy, between 2004 and 2006 under IRB approval and patient consent. Clinical and epidemiologic information is shown in Tables II and III. All women in the study population underwent preoperative clinical examination, ultrasound morphologic scoring (in all cases performed as a transvaginal examination, the abdominal approach was used when indicated), and color Doppler imaging. Samples were obtained from fasting patients either the day prior to, or the day of, surgical intervention before induction of anesthesia for treatment.

Table II. Clinical Features of Ovarian Cancer Patients

Age	Menopausal status	Ultrasound risk	Stage	Pathology
64	Post-	High	II	S. Bord.
63	Post-	High	IC	M. bord.
56	Post-	Unknown	IIA	Cl. C. Ca.
57	Post-	High	IA	Cl. C. Ca.
48	Post-	Intermediate	IA	M. ACa.
42	Pre-	High	IA	S. Bord.
24	Pre-	High	I	M. Bord.
24	Pre-	Intermediate	IA	S. Ca.
19	Pre-	Intermediate	I	M. ACa.
54	Post-	High	IIA	E. ACa.
58	Post-	High	IA	Cl. C. Ca.
28	Pre-	Intermediate	IA	M. Bord.
59	Post-	Intermediate	I	M. Bord.
58	Post-	Unknown	IC	S. ACa.
68	Post-	Low	IC	S. ACa.
36	Pre-	Low	IC	Unknown
33	Pre-	Unknown	IA	ACa.
53	Pre-	Unknown	IA	E. ACa.
59	Post-	High	IC	S. ACa.
29	Pre-	Low	IC	S. ACa.

Cl. C. Ca. clear cell carcinoma, ACa. adenocarcinoma, S. serous, E. ACa. endometrioid adenocarcinoma, M. mucinous

Table III. Clinical Information of Patient Affected by Benign Gynecological Disease

Age	Menopausal status	Ultrasound risk	Pathology
25	Pre	Intermediate	M.C.T.
21	Pre-	Intermediate	M.C.T.
39	Pre-	Intermediate	C. L. C.
39	Pre-	Intermediate	E. C.
36	Pre-	Intermediate	F. C.
68	Post-	Intermediate	S. CAD
50	Pre-	High	F. C.
55	Post-	Intermediate	S. Cad.
41	Pre-	Intermediate	Unknown
52	Pre-	Intermediate	M.C.T.
58	Post-	Intermediate	S. Cad.
52	Pre-	Intermediate	S. CAF.
65	Post-	Intermediate	M.C.T.
49	Pre-	Unknown	F. C.
28	Pre-	Unknown	D. C.
58	Post-	Unknown	S. CAF.
74	Post-	Unknown	M. CAD.
53	Unknown	Unknown	S. CAD.
48	Pre-	Low	S-M. Cad.
50	Post-	Low	S. Cad

M.C.T. mature cystic teratoma, *S. CAF* serous cystoadenofibroma, *F. C.* follicular cyst, *D. C.* dermoid cyst, *S. CAD.* serous cystoadenoma, *C. L. C.* corpus luteum cyst, *M. C.* mucinous cystoadenoma, *E. C.* endometriotic cyst, *S-M. Cad.* serous-mucinous cystoadenoma

Peptidome Capture and Isolation

Serum samples were centrifuged (7 min, 4°C, 16,100 rcf) and diluted 1:2 with 50 mM Tris-HCl, pH 7.0. Four hundred microliters of sera from ovarian cancer and benign controls was used per patient, and 200 µL of sera for pre- and post-prostatectomy specimens was used for biomarker discovery. Two chemokines, CCL28, known also as mucose-associated epithelial chemokine (MEC)m with a predicted MW 14 kDa (Antigenix America), and CXCL12 (Antigenix America), also known as SDF-1β with a predicted MW of 11 kDa, were added to the serum samples as internal process control standards. Pre-prostatectomy samples (200 µL aliquots) were spiked with CXCL12/SDF-1β and of CCL28/MEC at the concentration of 0.5 and 0.05 ng/µL, respectively, while 0.5 ng/µL of MEC and 0.05 ng/µL SDF-1β were added to the post-prostatectomy sera. Ovarian cancer patient samples were spiked with 0.5 ng/µL MEC and 0.05 ng/µL SDF-1β, as opposed to benign pelvic disease controls which were spiked with 0.05 ng/µL MEC and 0.5 ng/µL SDF-1β. Subsequently, nanoparticles were incubated with each diluted serum sample for 15 min at room temperature under slow rotation. After incubation and peptidome capture, samples were centrifuged (15 min, 25°C, 16,100 rcf), the supernatant was discarded, and the particles were washed two times by means of resuspending the pellets in 1 mL of the washing buffer (20% acetonitrile/0.5× PBS) and centrifuging (4 min, 25°C, 16,100 rcf). The pellet of washed particles, obtained as described above, was vortexed with 100 µL of elution buffer (60% acetonitrile/2% acetic acid) at room temperature. The elution mix was sonicated three times for 10 s each. The eluate was

saved. The elution step was repeated twice and the eluates pooled together. The eluates were then lyophilized until dry. The dried-up samples were stored at -20°C until use. Eluted proteins from the nanoparticles were reduced by dithiothreitol, alkylated by iodoacetamide, and digested by trypsin overnight at 37°C as described (27).

SDS-PAGE Analysis

The incubation of serum with particles has been performed as previously described (27). Serum, supernatant, and eluate derived from particle incubation were loaded on 4–20% Tris-Glycine gel (Invitrogen Corporation). Proteins were detected by Coomassie staining.

Mass Spectrometry Analysis

The peptides from each sample were analyzed by reversed-phase liquid chromatography/electrospray tandem mass spectrometry (MS/MS) using a linear trap quadrupole (LTQ)-Orbitrap mass spectrometer (Thermo Fisher Scientific, Waltham, MA) equipped with an in-line autosampler. The reverse-phase C18 column (0.5-mm i.d. × 50-mm length) was from Michrom BioResources. The column was washed for 2 min with mobile phase A (0.1% formic acid), and peptides were eluted using a linear gradient of 0% mobile phase B (0.1% formic acid, 80% acetonitrile) to 50% mobile phase B in 50 min at 2 µL/min, then to 100% B for an additional 2 min.

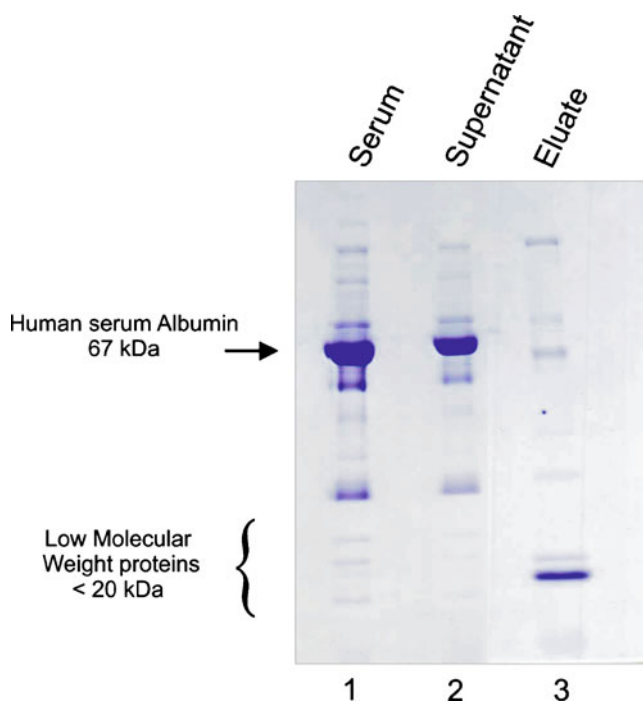


Fig. 1. SDS-PAGE analysis of human serum sample pre- and post-incubation with NIPAm/AAC nanoparticles. *Lane 1* Serum from healthy donor before incubation with particles. *Lane 2* Supernatant obtained after centrifugation of the mix of incubation containing serum and nanoparticles. *Lane 3* Eluate from nanoparticles: the samples are enriched in low-molecular-weight proteins, while albumin is mostly excluded

The mass spectrometer was operated in a data-dependent mode in which each full MS scan was followed by five MS/MS scans in which the five most abundant molecular ions were dynamically selected and fragmented by collision-induced dissociation using a normalized collision energy of 30%. To decrease carryover, one blank sample was analyzed using a 30-min, double high-performance liquid chromatograph (HPLC) gradient program after analyzing one sample. To verify HPLC reproducibility, two standard samples (yeast enolase digest, from Michrom BioResources) were analyzed using a 30-min HPLC program after analyzing 15 serum samples.

Bioinformatic Analysis

Protein identification was performed with SEQUEST. The data were searched against a fully tryptic indexed, human protein database maintained by the National Center for Biotechnology Information with a variable oxidized methionine and a static carboxyamidomethylated cysteine modification. Search results were filtered with the following criteria: minimum $X_{\text{Corr}}=2.2$ (+2), 3.5 (+3), minimum $dCn=0.1$, and a maximum precursor ion mass deviation of 15 ppm. An MS1-based comparative data analysis was accomplished using BioSieve (Thermo and Vast Scientific). Spectral counting (MS2-based) analysis was accomplished using Scaffold (Proteome Software, Inc. Portland, OR). Candidate differentially abundant peptides were evaluated by manual inspection of the raw data to confirm the peptide identifications, and differences in peptide relative abundances were determined using a two-

tailed t test applied to the spectral counts with the assumption of normally distributed data.

RESULTS

Particles Perform Size Exclusion and Concentration of Serum Proteins

In order to evaluate, in a qualitative manner, the efficiency of the nanoparticle capture methodology as a pre-processing step to eliminate the excess of high abundant proteins and concentrate the low-molecular-weight protein archive, a serum sample was processed and the starting sample, the post-particle supernatant, and eluate from particles were analyzed by SDS-PAGE. As shown in Fig. 1, in the eluate from particle (lane 3), the amount of albumin, and in general serum high abundant proteins, is tremendously reduced compared to the remaining albumin in the supernatant and starting raw sample. Conversely, the nanoparticle captured archive within the eluate reveals a number of highly concentrated and enriched proteins, which demonstrates the ability of particles to concentrate proteins based on the nature of the chemical bait used. Since the incubation of the sample was in pH values >3.5 , the acrylic acid bait is deprotonated and thus carries a negative charge, so the affinity of this particle type is most specific for positively charged polypeptides and proteins. Consequently, proteins/peptides that are negatively charged (such as those remaining in the supernatant), will not be captured by this specific nanoparticle.

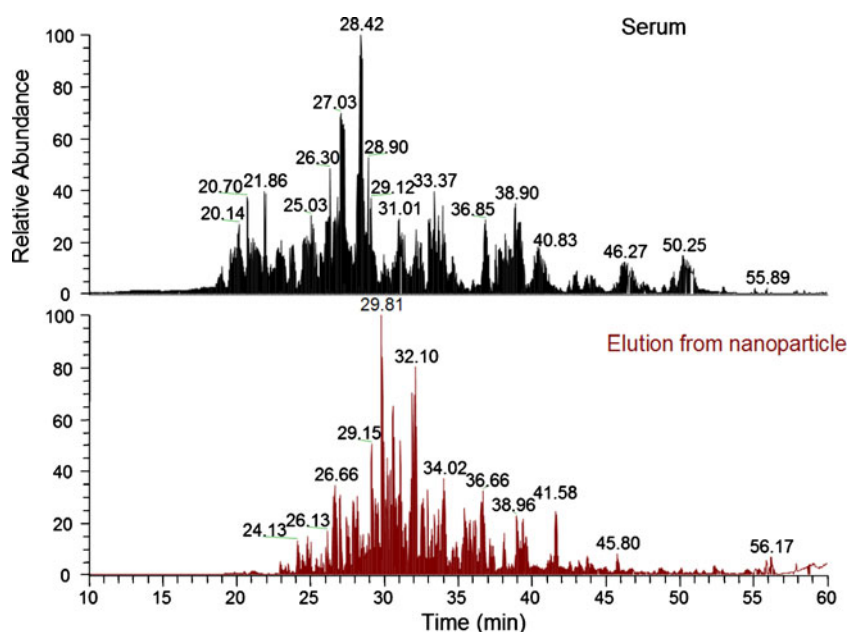


Fig. 2. Comparison of the LC-MS chromatography of serum and elution from nanoparticle. The abundant base peaks are labeled with their retention time. The peak intensities of albumin tryptic peptides such as AAFTECCQAADK (retention time 21.86 min), FQNALLVR (retention time 27.03 min), LVNEVTEFAK (retention time 28.42 min), KVPQVSTPTLVEVSR (retention time 28.90 min), RPCFSALEVDETYVPK (retention time 31.01 min), and AVMDDFAAFVEK (33.37 min) are high in the serum sample and are significantly low in the elution from nanoparticle sample

The nanoparticles' capacity to reduce albumin can be also seen by a qualitative analysis of a mass spectrometry chromatogram of raw serum and the nanoparticle eluate. As can be observed in Fig. 2 the peak intensities of several tryptic peptides of albumin, high in raw serum, are notably reduced in the elution from nanoparticle sample.

Evaluation of the Nanoparticle Capture-MS Workflow Performance

In order to evaluate the nanoparticle capture workflow's process performance and the reproducibility of the data, two chemokines, stromal cell-derived factor 1 β (SDF-1 β , also known as CCL12) and mucosae epithelial chemokine (MEC, known as CCL28), were spiked into the serum specimens before the nanoparticle processing step as internal standards.

The two chemokines were chosen because of their small size (in the MW range of the peptidomic archive under evaluation for this study) and their physicochemical properties (volatility and ionizability) for MS suitability, and the affinity for these two analytes for the specific nanoparticle bait molecule utilized has been previously demonstrated (27,28). SDF-1 β was added in a ratio of 10:1 in the pre-prostatectomy vs. post-prostatectomy samples and 1:10 in the cases vs. controls of the prostate cancer study set, while MEC was spiked in a ratio of 1:10 in the pre-prostatectomy vs. post-prostatectomy samples set and 10:1 in the ovarian cancer sera vs. controls samples. The chemokines were found to be differentially abundant with the expected ratio by BioSieve analysis (Fig. 3) in both study sets, and the MS data analysis confirmed the expected recovery of the internal standard controls. Since the levels of the endogenous, native CCL28 and CCL12 within

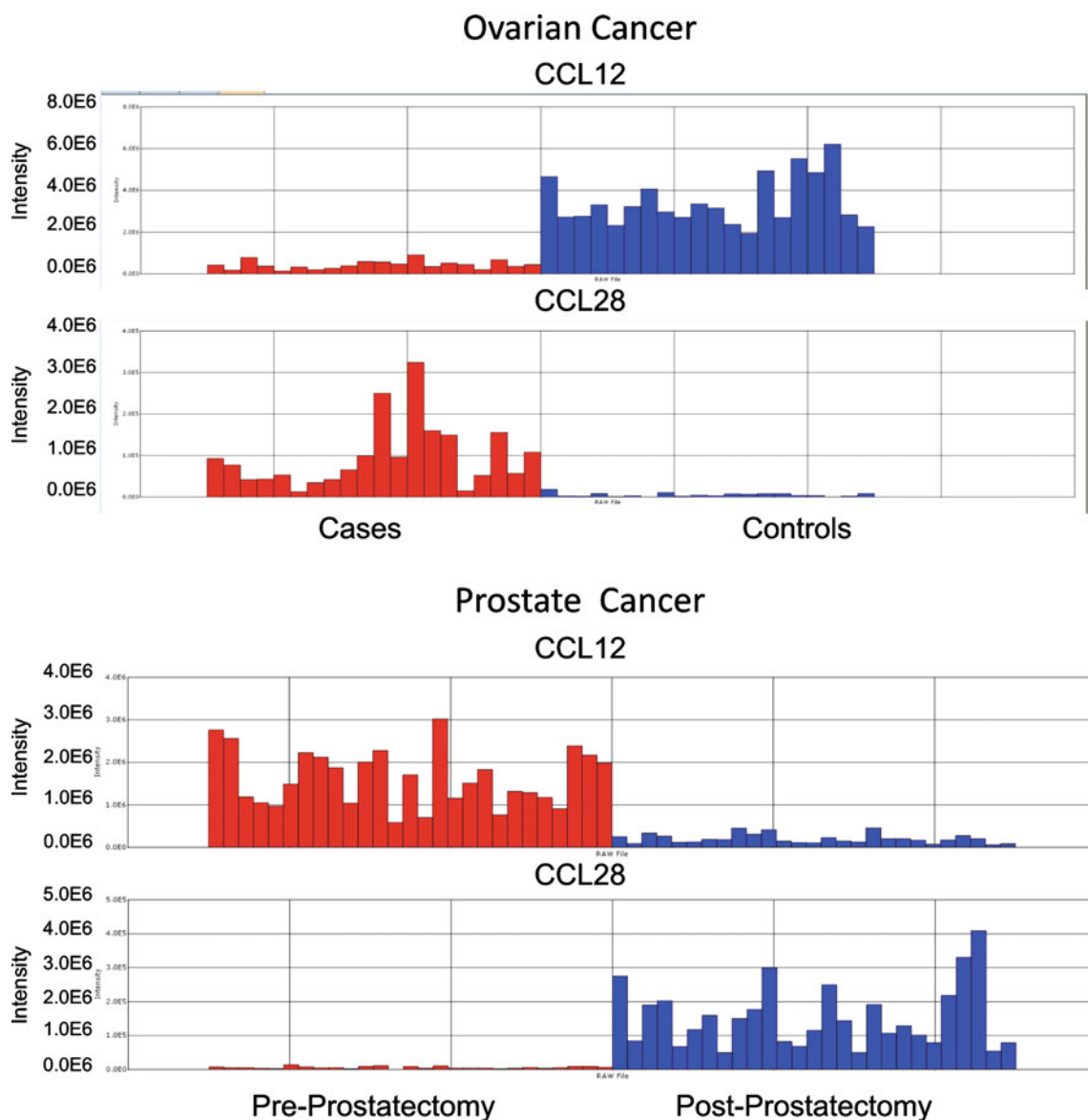


Fig. 3. Verification of nanoparticle capture workflow. The chemokines CCL12 and CCL28 were spiked, as internal standard process controls, in 1:10 and 10:1 ratios in ovarian cancer case and benign control sera, respectively (*top*), while in pre- and post-prostatectomy sera in the ratios of 10:1 and 1:10 (*bottom*). Each vertical bar in the histogram represents one serum sample from a cancer patient (*red*) or a control subject (*blue*), and the bar height corresponds to the peptide ion abundance measured

each patient sample are unknown and will vary from patient to patient, we can estimate the approximate reproducibility of the overall process by an analysis of the expected and actual ratios produced by the spiked-in chemokines over the population of samples rather than any one specific sample. The ratio of CCL12 intensity in the cases/controls of ovarian cancer is predicted to be 0.1 since a 1:10 amount was spiked in respectively and the experimentally derived value was 0.106. For CCL28, which was spiked in at 10:1 case vs. control, the

expected value of 10 compares to the actual value obtained of 10.052. For the prostate study, the ratio of CCL12 on the pre/post-prostatectomy samples resulted 8.592 compared to a theoretical value of 10, and for CCL28, the experimental value of 0.063 was determined compared to the theoretical value of 0.1. These results indicate excellent process reproducibility and variance across the entire set and provide increased confidence in the experimental results obtained for newly identified markers.

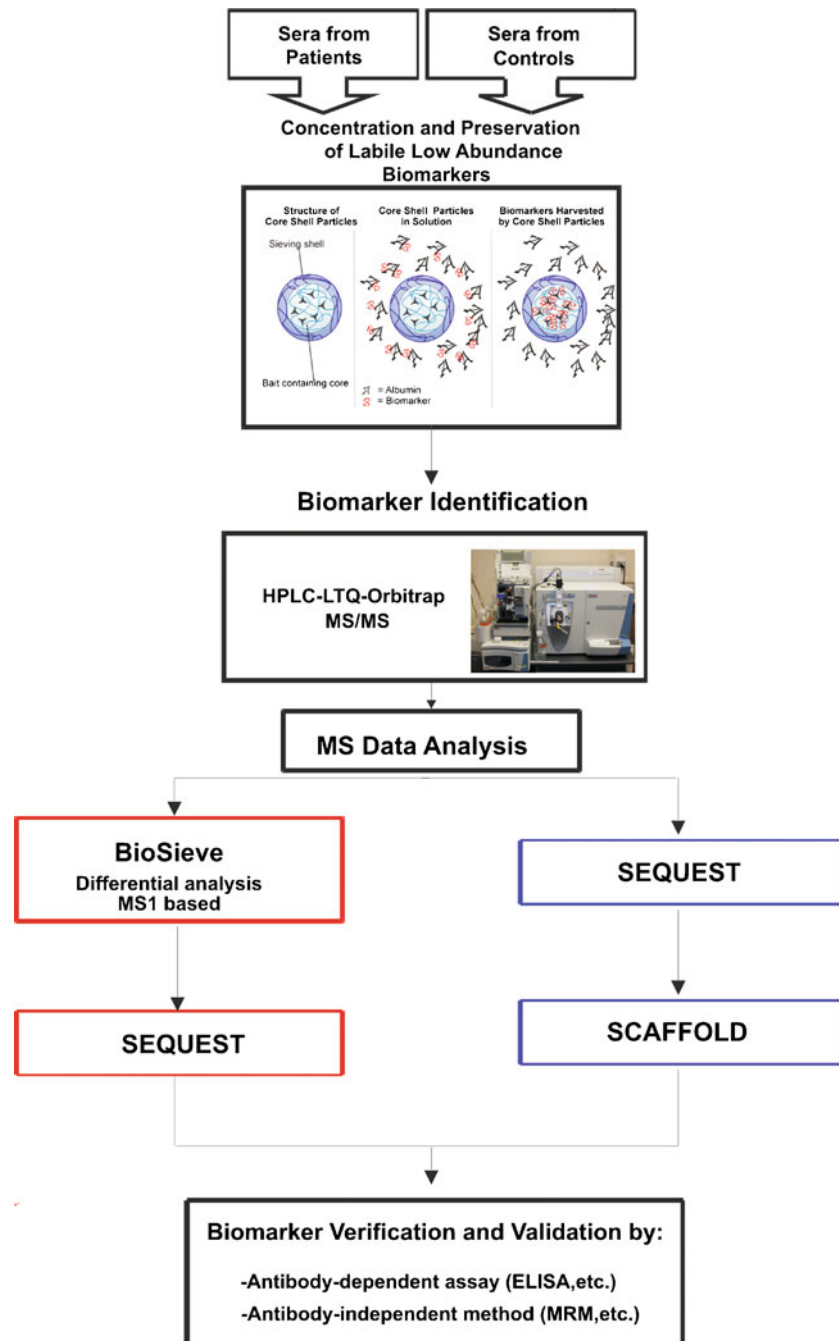


Fig. 4. Nanoparticle capture–mass spectrometry workflow. Sera from patients and controls are incubated with NIPAm/AAC particles, eluates from particles are analyzed by HPLC-LTQ-Orbitrap mass spectrometry, and the data analysis is performed using BioSieve and Scaffold software

Identification of Candidate CaP and OC LMW/Peptidome Biomarker Candidates Using Nanoparticle Capture-MS

In order to identify LMW protein/peptide serum biomarker candidates for CaP, 30 sera from 15 patients suffering from CaP, collected before radical prostatectomy and 6 weeks to 3 months following surgery (Table I), and 40 sera from gynecologic patients (20 samples from women affected by ovarian cancer and 20 samples from controls; Tables II and III) were subjected to our novel nanoparticle capture workflow followed by LC-MS/MS analysis (Fig. 4). The label-free spectral counting Scaffold analyses of MS/MS data from the nanoparticle-captured protein analytes yielded the determination of 14 proteins with higher abundance in the pre-prostatectomy samples compared to the post-prostatectomy samples (Table IV) and 59 proteins with higher abundance in the early-stage OC sample compared to the age-matched benign gynecologic controls (Table V). Only analytes whose spectral counts achieved at least a 50% differential amount were included in these tables. Highlighted in red are the spiked-in internal standard proteins that, as expected, were found by both BioSieve and Scaffold (shown) to be differentially abundant. This result reveals that the entire process produces the expected results, thus providing increased confidence in the new experimentally determined candidate biomarker proteins. To provide a better sense of the complexity of the samples after preprocessing with nanoparticles, the total number of proteins and peptides that have been identified on average for the group of case/controls in the ovarian cancer or pre/post-prostatectomy in the prostate cancer study are shown in Table VI.

Moreover, a list of the most abundant proteins identified in the prostate and ovarian sets samples are reported (Tables VII and VIII). Proteins such as albumin and complement component 3 are still the most abundant proteins regardless of upfront preprocessing. It is important to consider that a nanoparticle-based sample preparation is not a depletion-based approach but

is an enrich-based strategy to “amplify” and concentrate low molecular analytes; thus, the spectral counts of the albumin and complement component 3 peptides are dramatically reduced and the ratios of the endogenous high abundance analytes to the newly discovered analytes is lower. Due to the extraordinarily high abundance of proteins such as albumin that exist in one to ten million-fold molar excess to low abundance proteins, it would be impossible to completely eliminate them from downstream analysis. Since mass spectrometry works in a dynamic range of four to five orders of magnitude, the reduction of a consistent part of the most abundant protein (as showed in the gel) still provides a great advantage in this analysis, allowing the identification of the less abundant peptides/proteins that usually are masked.

In order to determine, within the proteins identified, candidate molecules that could be more specific for prostate cancer and ovarian cancer and thereby produce more specific markers for further analysis and validation, the candidates obtained from the two study sets were compared. The results of the analysis (Fig. 5 and Table IX) revealed a series of proteins whose increased relative abundance, as determined by label-free spectral counting methodology, was either CaP-specific or OC-specific. Comparison of the list of ovarian cancer candidates to biomarker candidates discovered using the identical workflow applied to serum sets from patients with prostate cancer revealed only a marginal overlap, indicating potential for specificity in the candidates uncovered to date.

Comparing the results from different neoplastic processes could be a useful means to identify proteins involved more specifically in the neoplastic process of the specific type of tumor (i.e., ovarian cancer vs. prostate cancer) vs. those that may be more reflective of any neoplastic growth or inflammatory process. Manual verification vitronectin precursor and leucin-rich alpha-2-glycoprotein 1, taken as a representative example of differentially abundant analytes for CaP (Fig. 6a) and OC (Fig. 6b), are shown and reveal that the MS/MS analysis was correct for these example candidate biomarkers, providing increased confidence in the Scaffold results.

Table IV. Scaffold Spectral Count Analysis of Differentially Abundant Analytes Elevated in the Serum of Pre-prostatectomy Patients Compared to Patient Matched Post-prostatectomy Patients

Protein ID	Description	Pre ^a	Post ^b	Relative difference (%) ^c
gil55956899 reflNP_000217.2	Keratin 9	32	19	51.0
gil4502153 reflNP_000375.1	Apolipoprotein B precursor	55	32	52.9
gil50659080 reflNP_001076.2	Serpin peptidase inhibitor, clade A, member 3 precursor	28	15	60.5
gil88853069 reflNP_000629.3	Vitronectin precursor	4	2	66.7
gil4557287 reflNP_000020.1	Angiotensinogen preproprotein	11	5	75.0
gil4504315 reflNP_003536.1	H4 histone family, member J	10	4	85.7
gil4504489 reflNP_000403.1	Histidine-rich glycoprotein precursor	5	2	85.7
gil4503745 reflNP_001447.1	Filamin 1 (actin-binding protein-280)	10	3	107.7
gil76563933 reflNP_001029058.1	Chemokine (C-X-C motif) ligand 12 (stromal cell-derived factor 1) isoform gamma	224	62	113.3
gil47132551 reflNP_997640.1	Fibronectin 1 isoform 2 preproprotein	4	1	120.0
gil9257232 reflNP_000598.1	Orosomucoid 1 precursor	9	2	127.3
gil4502511 reflNP_001728.1	Complement component 9	15	3	133.3
gil16753233 reflNP_006280.2	Talin 1	10	2	133.3
gil4757960 reflNP_004351.1	Cadherin 1, type 1 preproprotein	5	0	200.0

^a Sum of spectra found in all the pre-prostatectomy samples

^b Sum of spectra found in all the post-prostatectomy serum samples

^c Relative difference = ((Pre - Post)/Average of number of spectra for the Pre and Post) × 100

Table V. Scaffold Spectral Count Analysis of Differentially Abundant Analytes Elevated in the Serum of Early Stage Ovarian Cancer Patients Compared to Patients with Benign Gynecologic Conditions

Protein ID	Description	Case ^a	Controls ^b	Relative difference (%) ^c
gil2253881 reflNP_683513.1	Chemokine (C-C motif) ligand 28 precursor	29	0	200.0
gil88758615 reflNP_000410.2	Integrin alpha 2b preproprotein	28	0	200.0
gil13562114 reflNP_110400.1	Beta tubulin 1, class VI	17	0	200.0
gil41281905 reflNP_848537.1	UNC-112 related protein 2 long form	14	0	200.0
gil7669550 reflNP_054706.1	Vinculin isoform meta-VCL	13	0	200.0
gil4502153 reflNP_000375.1	Apolipoprotein B precursor	358	3	196.7
gil47132551 reflNP_997640.1	Fibronectin 1 isoform 2 preproprotein	226	3	194.8
gil16753233 reflNP_006280.2	Talin 1	73	2	189.3
gil4503745 reflNP_001447.1	Filamin 1 (actin-binding protein-280)	65	4	176.8
gil31652249 reflNP_004130.2	Lipopolysaccharide-binding protein precursor	28	2	173.3
gil4503643 reflNP_000121.1	Coagulation factor V precursor	20	2	163.6
gil4501891 reflNP_001093.1	Actinin, alpha 1	16	2	155.6
gil17921989 reflNP_005991.1	Tubulin, alpha 1	21	4	136.0
gil4557287 reflNP_000020.1	Angiotensinogen preproprotein	15	3	133.3
gil4557485 reflNP_000087.1	Ceruloplasmin (ferroxidase)	75	16	129.7
gil4502067 reflNP_001624.1	Alpha-1-microglobulin/bikunin precursor	9	2	127.3
gil4502511 reflNP_001728.1	Complement component 9	62	15	122.1
gil21735614 reflNP_003652.2	Apolipoprotein L1 isoform a precursor	16	4	120.0
gil73858568 reflNP_000053.2	Complement component 1 inhibitor precursor	104	27	117.6
gil55770842 reflNP_000558.2	C-reactive protein, pentraxin-related	15	4	115.8
gil16418467 reflNP_443204.1	Leucine-rich alpha-2-glycoprotein 1	9	3	100.0
gil55956899 reflNP_000217.2	Keratin 9	112	38	98.7
gil4501887 reflNP_001605.1	Actin, gamma 1 propeptide	72	30	82.4
gil4504781 reflNP_002206.1	Inter-alpha (globulin) inhibitor H1	9	4	76.9
gil4502161 reflNP_001637.1	Apolipoprotein C-IV	10	5	66.7
gil40317626 reflNP_003237.2	Thrombospondin 1 precursor	157	83	61.7
gil4505981 reflNP_002695.1	Pro-platelet basic protein precursor	67	39	52.8
gil62912466 reflNP_001017366.1	Complement component 4 binding protein, beta chain isoform 2 precursor	22	13	51.4
gil50659080 reflNP_001076.2	Serpin peptidase inhibitor, clade A, member 3 precursor	70	42	50.0
gil8922987 reflNP_060856.1	PCI domain containing 2	3	0	200.0
gil19923106 reflNP_000437.3	Paraoxonase 1	3	0	200.0
gil21361302 reflNP_006206.2	Serine (or cysteine) proteinase inhibitor, clade A (alpha-1 antiproteinase, antitrypsin), member 4	3	0	200.0
gil4507021 reflNP_000333.1	Solute carrier family 4, anion exchanger, member 1	3	0	200.0
gil89027630 reflXP_941134.1	PREDICTED: similar to actin-related protein 3-beta isoform 1 isoform 3	3	0	200.0
gil4505879 reflNP_002655.1	Pleckstrin	3	0	200.0
gil22035665 reflNP_055874.1	Talin 2	3	0	200.0
gil70906435 reflNP_005132.2	Fibrinogen, beta chain preproprotein	3	0	200.0
gil34577083 reflNP_689937.2	Ras suppressor protein 1 isoform 2	4	0	200.0
gil113420458 reflXP_941447.2	PREDICTED: similar to Protein FAM82B	4	0	200.0
gil47419932 reflNP_000164.3	Platelet glycoprotein Ib alpha polypeptide precursor	5	0	200.0
gil54112429 reflNP_212132.2	Dedicator of cytokinesis 7	5	0	200.0
gil4503631 reflNP_000120.1	Coagulation factor XIII A1 subunit precursor	6	0	200.0
gil4557443 reflNP_000069.1	Cholesteryl ester transfer protein, plasma precursor	7	0	200.0
gil5031635 reflNP_005498.1	Cofilin 1 (non-muscle)	8	1	155.6
gil73858566 reflNP_000176.2	Heparin cofactor II precursor	6	1	142.9
gil34335256 reflNP_003808.1	A disintegrin and metalloproteinase domain 7	4	1	120.0
gil45580723 reflNP_066275.3	Haptoglobin-related protein	4	1	120.0
gil4502261 reflNP_000479.1	Serine (or cysteine) proteinase inhibitor, clade C (antithrombin), member 1	3	1	100.0
gil70778918 reflNP_002207.2	Inter-alpha globulin inhibitor H2 polypeptide	3	1	100.0
gil31982945 reflNP_689564.2	Solute carrier family 5 (sodium/glucose cotransporter), member 10	3	1	100.0
gil4557391 reflNP_000057.1	Complement component 8, beta polypeptide preproprotein	3	1	100.0
gil94721347 reflNP_006656.2	Heparanase	3	1	100.0
gil4507357 reflNP_003555.1	Transgelin 2	3	1	100.0
gil21361820 reflNP_064538.2	Hypothetical protein LOC56912	4	2	66.7
gil14917119 reflNP_066293.2	Keratin 34	4	2	66.7
gil20336724 reflNP_115809.1	Zinc finger protein 333	6	3	66.7
gil31559819 reflNP_853515.1	Keratin 25C	6	3	66.7

Table V. (continued)

gil21735625 reflNP_663723.1	Tyrosine 3/tryptophan 5-monoxygenase activation protein, zeta polypeptide	5	3	50.0
gil14917115 reflNP_002268.2	Keratin 31	5	3	50.0

^a Case = sum of spectra founded in all the case samples

^b Control = sum of spectra founded in all the Control samples

^c Relative difference = ((Case - Control)/Average of number of spectra for the Case and the Control) × 100

DISCUSSION

The search for novel clinically relevant disease-specific protein biomarkers that can be measured in an easily accessible body fluid such as the blood remains a huge challenge for researchers because of the complexity of the circulatory proteome and the likely extremely low concentration of any candidate biomarkers coupled with the lability of the markers *in vivo* and *ex vivo*. The intensity of biomarker discovery efforts has led to the increased investigation of the peptidome/LMW proteome because of the facile nature of this archive to easily pass between the tissue and bloodstream. This information archive may be especially a rich source of disease-specific information for the early detection of cancer, toxicity, and drug abuse/doping whereby complex changes within the tissue microenvironment may be reflected in altered pathophysiology of the affected organ(s).

To that end, we developed a novel workflow for LMW proteome/peptidome biomarker research of low-molecular-weight proteins/peptides by the novel application of hydrogel nanoparticle technology as a tool to rapidly capture and concentrate analytes in solution coupled with high-sensitivity mass spectrometry analysis (Fig. 4). The novel aspect of this new biomarker discovery method lies within the capacity of the core-shell nanoparticles (described in (26–28)) to perform both an affinity capture step and size exclusion chromatography in solution in just one step. In this instance, we used an acrylic acid affinity capture reagent that is immobilized within the core region of the nanoparticle, which is then covered with a shell matrix with tuned porosity to allow in analytes <30 kDa.

Consequently, for this feasibility study, the particles will bind only protein analytes that are net positively charged at the buffered pH of 7.0. Other marker capture nanoparticles with different affinity “baits” can be easily constructed with other types of affinity dye reagents, for example Cibacron blue dye which we showed could effectively capture 100% of hGH in urine (27). The ability of the particles to perform two-

Table VI. Total Peptide and Protein Count for Ovarian and Prostate Sample Set Obtained by Scaffold

		Peptides	Proteins
Ovarian cancer	Case	569	126
	Control	513	118
Prostate cancer	Pre-prostatectomy	271	36
	Post-prostatectomy	266	35

An average number of protein and peptides for all the case, controls, and pre- and post-prostatectomy have been calculated

dimensional separation in just one step, whereby subsets of the peptidome (in this case the positively charged archive) are captured from hundreds of microliters of serum along with excluding all of the high abundance resident proteins such as albumin and immunoglobulins, provides a concentration step that is equivalent to injecting in 400 μL (for ovarian cancer study) and 200 μL (for prostate cancer study) into the Orbitrap at once, without the need for any of the types of pre-fractionation step normally required to analyze blood proteins by mass spectrometry (29). Most of the procedures commonly used can result in the loss of part of important information, either because many LMW serum proteins are bound to high-molecular-weight carrier proteins or because of lengthy sample handling procedures. Moreover, mass spectrometry normally works in a dynamic range of three to four orders of magnitude, meaning that highly abundant proteins such as albumin mask most of the lower abundance proteins.

We applied the nanoparticle-based biomarker capture technique for the determination of differentially abundant peptidomes from two important human cancers as a feasibility case study and not a definitive biomarker discovery effort. We utilized a unique set of pretreatment serum samples taken from CaP patients with organ-confined disease who were undergoing radical prostatectomy whereby patient-matched pre- and post-prostatectomy samples were obtained. This type of serum collection represents a powerful opportunity to understand the changes in protein expression from the same individual with and without organ-confined cancer. We utilized a second study set serum obtained from women with early-stage ovarian cancer and women with benign

Table VII. Protein Identified as Most Abundant in Prostate Cancer Pre-prostatectomy and Post-prostatectomy Samples

Protein identify as most abundant in prostate cancer study	MW
Albumin precursor (<i>Homo sapiens</i>)	69
Complement component 3 precursor (<i>Homo sapiens</i>)	187
Apolipoprotein A-I preproprotein (<i>Homo sapiens</i>)	31
Apolipoprotein A-IV precursor (<i>Homo sapiens</i>)	45
Transferrin (<i>Homo sapiens</i>)	77
Complement component 4A preproprotein (<i>Homo sapiens</i>)	193
Serine (or cysteine) proteinase inhibitor, clade A (alpha-1 antiproteinase, antitrypsin), member 1 (<i>Homo sapiens</i>)	47
Apolipoprotein E precursor (<i>Homo sapiens</i>)	36
Platelet factor 4 (chemokine (C-X-C motif) ligand 4; <i>Homo sapiens</i>)	11
Complement component 1, r subcomponent (<i>Homo sapiens</i>)	80

Table VIII. Protein Identified as Most Abundant in Ovarian Cancer and Controls Samples

Protein identify as most abundant in ovarian cancer study	MW
Albumin precursor (<i>Homo sapiens</i>)	69
Complement component 3 precursor (<i>Homo sapiens</i>)	187
Complement component 4A preproprotein (<i>Homo sapiens</i>)	193
Apolipoprotein A-I preproprotein (<i>Homo sapiens</i>)	31
Transferrin (<i>Homo sapiens</i>)	77
Complement component 1, r subcomponent (<i>Homo sapiens</i>)	80
Platelet factor 4 (chemokine (C-X-C motif) ligand 4; <i>Homo sapiens</i>)	11
Serine (or cysteine) proteinase inhibitor, clade A (alpha-1 antiproteinase, antitrypsin), member 1 (<i>Homo sapiens</i>)	47
Apolipoprotein A-II preproprotein (<i>Homo sapiens</i>)	11
Apolipoprotein C-III precursor (<i>Homo sapiens</i>)	11

gynecologic conditions as an age-matched control group. The use of differentially spiked-in cytokine standards into the starting serum sample that were then analyzed at the end of the entire process by MS/MS allowed us to evaluate the robustness of the overall process, with all samples showing the expected 10:1 or 1:10 ratios as seen by BioSieve analysis (Fig. 3). While each individual independently run sample did not show the expected ion abundance ratios for peptides corresponding to the two spiked proteins, the average of the case and control sample ratios was approximately equal to the expected ratios and indicated overall process fidelity. Based on this result, we have higher confidence in the biomarker candidate information generated by MS/MS and differential spectral counting methods within the cancer study sets utilized. Furthermore, to evaluate the specificity of the candidate markers found by nanoparticle harvesting, we compared the resultant candidates within the two cancers to each other. We used the results of both Scaffold and BioSieve software, the former to analyze the MS2 data and the other to analyze the MS1 data and integrate the information from both methods. An interesting aspect of a MS1-based approach is that the comparison is not related to an MS2 identification, and as long as the independent MS chromatograms align well, the software performs a statistically driven analysis on any reproducibly seen peak without regard to whether or not an MS2 spectrum is not available, and thus, lower abundant analytes are also analyzed. Peptides that are found to be potentially differentially abundant can then be identified searching the obtained MS2 data against a human protein database (NCBI) with SEQUEST. An MS targeting experiment could be performed when the MS2 spectra were not obtained from the first analysis and differentially abundant peptides taken forward for further validation by mass spectrometry-based methods such as multiple reaction monitoring (MRM).

We chose a label-free spectral counting approach since this method has been found to provide a cost-efficient reproducible means of obtaining accurate differences in relative peptide abundances between different input samples based on the differences in the number of times a specific tryptic fragment is selected for MS/MS within a data-dependent experiment (30).

An overview of the proteins identified for both OC and CaP, found by either Scaffold (results shown in Tables IV and V)

or Biosieve (not shown) and in aggregate summary of both (Table IX), reveals low-molecular-weight protein such as Profilin 1, Ras suppressor protein 1, S100A7, Ribonuclease RNase Family, Platelet factor 4, and enzymes. The nanoparticles captured LMW fragments of high-molecular-weight proteins (e.g., ceruloplasmin, fibronectin 1, Talin 1, actinin alpha 1, apolipoprotein B) that were found to be differentially abundant in cancer vs. control sera as defined by spectral counting differences. The inferred proteins, corresponding to identified peptides, included serum plasma proteins such as serpin peptidase inhibitor, clade A, member 3 precursor, angiotensinogen, and orosomucoid 1. The identified tryptic fragments originate from both cytoplasmic and nuclear proteins which reinforce the value of the LMW proteome/peptidome as being populated by cellular information, reflecting ongoing tissue pathophysiology. The presence in the serum of peptide fragments of intracellular proteins may yield valuable information about the processes and signaling networks operating within the tumor cells. Integrins, LRG, and LPB have been identified in this pilot study as proteins differentially abundant uniquely in ovarian cancer. Integrins constitute a family of transmembrane receptor proteins that mediate the extracellular matrix influence on cell growth and differentiation (31–34). Decreased or increased integrin expression has been shown to be associated with cytoskeletal changes coincident with tumor transformation, and a role for integrins in tumor growth and metastasis has repeatedly been proposed (35–38).

If these results are extensively validated in larger independent study sets, development of the expression profiles of LMW peptide fragments of integrin might be useful as tumor progression markers for prognostic and for diagnostic purposes. Moreover, for individual tumors, this may have further potential in identifying a cell surface signature for a specific tumor type and/or stage. (39). Leucine-rich alpha-2-glycoprotein-1 (LRG) is a serum glycoprotein of unknown function that has shown promise based on qualitative assessments as a biomarker for certain diseases, including microbial infections and cancer (40–42).

Increased serum LRG was observed in patients with several types of cancer, including pancreatic (43), liver (44), lung (45), and epithelial ovarian cancers (46,47). However, the lack of a quantitative assay for LRG has so far limited its application. (48). Lipopolysaccharide-binding protein gene

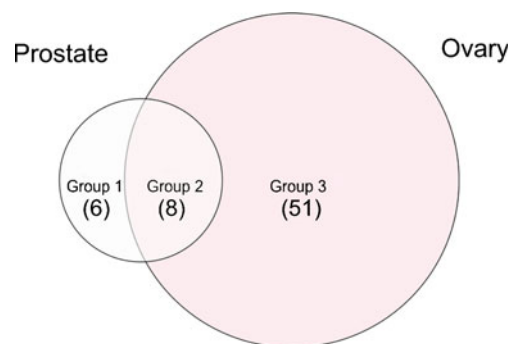


Fig. 5. Venn diagram visualization of group 1 (CaP-specific proteins; increased spectral counts in pre- vs. post-prostatectomy serum) not found upregulated in OC; group 3 (OC-specific proteins; increased spectral counts in OC vs. benign control) not found upregulated in CaP; and group 2 commonly upregulated proteins in both CaP and OC

Table IX. Summary List of Nanoparticle-Captured Analytes

Group 1 (prostate) ^a	Group 2 (common) ^b	Group 3 (ovary) ^c
Cadherin 1, type 1 preproprotein	Angiotensinogen preproprotein	Actin, gamma 1 propeptide
H4 histone family, member J	Apolipoprotein B precursor	Actinin, alpha 1
Histidine-rich glycoprotein precursor	Complement component 9	Alpha-1-microglobulin/bikunin precursor
Orosomucoid 1 precursor	Fibronectin 1 isoform 2 preproprotein	Apolipoprotein C-IV
Vitronectin precursor	Filamin 1 (actin-binding protein-280)	Apolipoprotein L1 isoform a precursor
Chemokine (C-X-C motif) ligand 12	Keratin 9	Beta tubulin 1, class VI
	Serpin peptidase inhibitor, clade A, member 3 precursor	Ceruloplasmin (ferroxidase)
	Talin 1	Cholesteryl ester transfer protein, plasma precursor
		Chemokine (C-C motif) ligand 28 precursor
		Coagulation factor V precursor
		Coagulation factor XIII A1 subunit precursor
		Cofilin 1 (non-muscle)
		Complement component 1 inhibitor precursor
		Complement component 4 binding protein, beta chain isoform 2 precursor
		C-reactive protein, pentraxin-related
		Dedicator of cytokinesis 7
		Fibrinogen, beta chain preproprotein
		Integrin alpha 2b preproprotein
		Inter-alpha (globulin) inhibitor H1
		Leucine-rich alpha-2-glycoprotein 1
		Lipopolysaccharide-binding protein precursor
		Paraoxonase 1
		PCI domain containing 2
		Platelet glycoprotein Ib alpha Polypeptide precursor
		Pleckstrin
		PREDICTED: similar to actin-related protein 3-beta isoform 1 isoform 3
		PREDICTED: similar to Protein FAM82B
		Pro-platelet basic protein precursor
		Ras suppressor protein 1 isoform 2
		Serine (or cysteine) proteinase inhibitor, clade A (alpha-1 antiproteinase, antitrypsin), member 4
		Solute carrier family 4, anion exchanger, member 1
		Talin 2
		Thrombospondin 1 precursor
		Tubulin, alpha 1
		UNC-112 related protein 2 long form
		Vinculin isoform meta-VCL
		Heparin cofactor II precursor
		A disintegrin and metalloproteinase domain 7
		Haptoglobin-related protein
		Serine (or cysteine) proteinase inhibitor, clade C (antithrombin), member 1
		Inter-alpha globulin inhibitor H2 polypeptide
		Solute carrier family 5 (sodium/glucose cotransporter), member 10
		Complement component 8, beta polypeptide preproprotein
		Heparanase
		Transgelin 2
		Hypothetical protein LOC56912
		Keratin 34
		Zinc finger protein 333
		Keratin 25C
		Tyrosine 3/tryptophan 5-monooxygenase activation protein, zeta polypeptide
		Keratin 31

^a Group 1: CaP-specific (elevated in CaP, not found in OC)^b Group 2: elevated in both CaP and OC^c Group 3: OC-specific (elevated in OC, not found in CaP). Only those analytes whose total spectral counts were different by >50% relative to the matched control group are shown (pre- vs. post-prostatectomy for CaP and cancer vs. benign for OC)

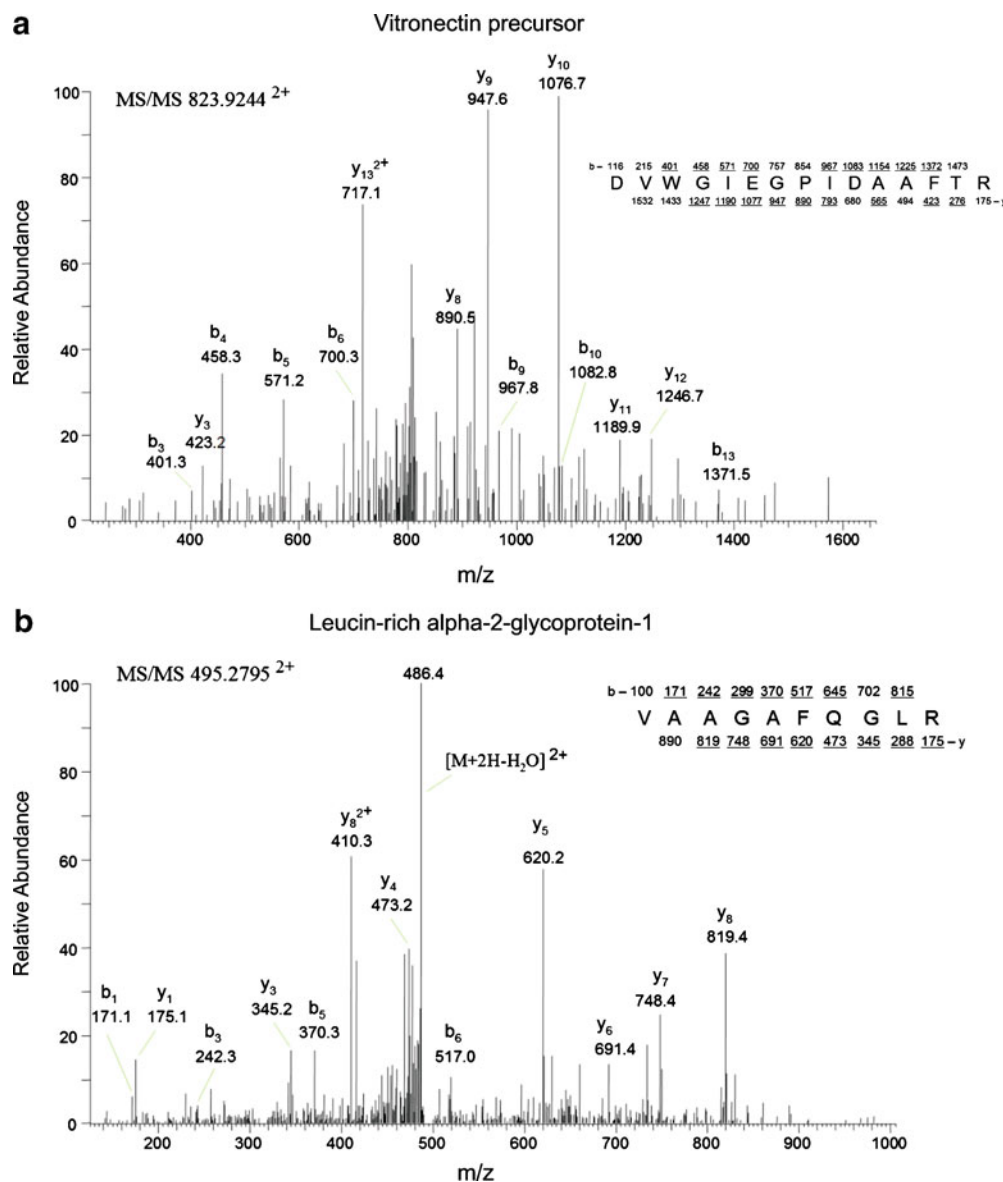


Fig. 6. MS/MS spectra for peptide analytes with statistically significant elevations. The precursor b and y ion masses are shown, as well as the matched amino acid sequence (*top right for each panel*) for MS/MS spectra corresponding to **a** a CaP-specific peptide from vitronectin precursor and **b** an OC-specific peptide from leucine-rich alpha 2 glycoprotein 1

has been found upregulated in clear cell ovarian cancer compared to other major histological types (49).

Differentially abundant peptides/LMW fragments found in the prostate cancer study set include proteins already correlated with carcinogenesis or prostate cancer. Vitronectin and cadherin 1 are cell adhesion proteins whose involvement in cancer progression and cellular spreading has been investigated and demonstrated (50,51). Vitronectin is recognized by certain members of the integrin family and acts as cell-to-substrate adhesion molecule, while cadherin 1 is involved in mechanisms regulating cell-cell adhesions, mobility, and proliferation of epithelial cells (52,53). The presence of vitronectin and cadherin 1 in the circulation could indicate the local loss of diffusion barriers, such as cell junction and the basement membrane. (54). Vitronectin has recently been identified as an extrinsic inducer of stem cell differentiation

through an integrin alpha(v)beta(3)-dependent mechanism (55) and may be important in mediating bone metastasis in CaP (56). Moreover, high expression levels of cadherin 1 fragment in serum have been observed in advanced metastatic prostate cancer (57,58).

The spiked-in internal standard standards, MEC and SDF-1, were both found to be differentially abundant in the correct expected pattern by both Scaffold (shown) and BioSieve (not shown), which provides increased confidence to the validity of the newly identified LMW candidates found. Of course, further analysis will be required for full validation. Future work will encompass antibody-based (e.g., ELISA) and antibody-independent (MRM-MS) verification and validation of differential expression in independent blinded serum study sets, including benign and inflammatory diseases as well as other cancers, to understand the

specificity and sensitivity of each candidate alone and in combination with each other.

Overall, we identified more differentially abundant proteins in the OC study sets than with CaP samples, and this is very likely due to the fact that we used a smaller input starting volume of serum for CaP studies (due to limitations in sample available) compared to OC samples. This is in keeping with expected results from nanoparticle capture since the entire contents are analyzed from the particle eluates: more input sample, more LMW peptidome analyzed/MS run. Consequently, it is highly likely that the number of CaP-specific candidates would increase if input starting sample volume increased. Moreover, this then highlights the potential for this workflow to enable detection of lower level endogenous proteins and protein fragments as larger volumes of starting sample are used. To that end, among other investigations, we are evaluating experimental results whereby very large volumes (e.g., 8 cc) of body fluids such as serum are used as the input into the nanoparticle capture workflow. The results described in this study are not meant in any way to reflect a comprehensive analysis of the serum peptidome or the entirety of the prostate and ovarian cancer LMW biomarker candidates that exist. Indeed, the identified analyte content is entirely dependent on the bait chemistry used within the nanoparticle. We used an acrylic acid capture chemistry that will selectively bind only analytes with a net positive charge at pH 7.0. Of course, the charge structure of the LMW analyte is dependent on the amino acid composition of the peptide/LMW protein. In the future, one can imagine the use of cocktails of particles with differential binding chemistries for positively charged proteins, negatively charged proteins, phosphoproteins, glycoproteins, etc. that will provide larger screening capabilities and wider coverage of the peptidome for biomarker discovery.

CONCLUSIONS

With this work, we have begun to test a novel workflow for body fluid-based biomarker discovery based on the application of a novel nanoparticle-based biomarker capture and concentration technology to amplify, fractionate, and enrich the peptidome/LMW analytes in a single simple step that in just a few minutes can harvest candidate biomarker analytes from raw unprocessed serum. This workflow provides subsequent high-resolution RPLC-MS/MS analysis with a concentrated and fractionated sample enriched for peptidome content. Using this approach, we have identified an initial set of OC and CaP-specific candidate peptides/LMW proteins from what appears to be a rich source of information. These candidates will require further extensive verification and validation in order to understand clinical utility either alone or in combination.

ACKNOWLEDGMENTS

The authors appreciate the generous support of Dr. Vikas Chandhoke and the Department of Life Sciences at George Mason University. This work was partly supported by the Italian Istituto Superiore di Sanita` in the framework Italy/USA cooperation agreement between the U.S. Depart-

ment of Health and Human Services, George Mason University, and the Italian Ministry of Public Health. This work was partially supported by the U.S. Department of Energy grant no. 201270.

REFERENCES

1. Crawford ED. Understanding the epidemiology, natural history, and key pathways involved in prostate cancer. *Urology*. 2009;73 Suppl 5:4-10.
2. Barry MJ. Clinical practice. Prostate-specific-antigen testing for early diagnosis of prostate cancer. *N Engl J Med*. 2001;344:1373-7.
3. Schröder FH, Hugosson J, Roobol MJ, ERSPC Investigators, *et al*. Screening and prostate-cancer mortality in a randomized European study. *N Engl J Med*. 2009;360:1320-8.
4. Roehrborn CG. The utility of serum prostatic-specific antigen in the management of men with benign prostatic hyperplasia. *Int J Impot Res*. 2008;20 Suppl 3:S19-26.
5. Thompson IA, Pauler DK, Goodman PJ, *et al*. Prevalence of prostate cancer among men with a prostate-specific antigen level of ≤ 4.0 ng per milliliter. *N Engl J Med*. 2004;350:2239-46.
6. Horner MJ, Ries LAG, Krapcho M, *et al*, editors. SEER Cancer Stat Fact Sheets. 2009, Bethesda, MD. National Cancer Institute. <http://seer.cancer.gov/statfacts/html/ovary.html>, accessed December 2, 2009.
7. Rosenthal AN, Menon U, Jacobs IJ. Screening for ovarian cancer. *Clinical Obstetrics and Gynecology*. 2006;49:433-47.
8. Duffy MJ, Bonfrer JM, Kulpa J, *et al*. CA125 in ovarian cancer. European Group on Tumor Markers guidelines for clinical use. *Int J Gynecol Cancer*. 2005;15:679-91.
9. Bast Jr RC. Status of tumor markers in ovarian cancer screening. *J Clin Oncol*. 2003;21 Suppl 10:200s-5s.
10. Azad NS, Rasool N, Annunziata CM, Minasian L, Whiteley G, Kohn EC. Proteomics in clinical trials and practice: present uses and future promise. *Mol Cell Proteomics*. 2006;5:1819-29.
11. Buys SS, Partridge E, Greene MH, *et al*. Ovarian cancer screening in the prostate, lung, colorectal and ovarian (PLCO) cancer screening trial: findings from the initial screen of a randomized trial. *Am J Obstet Gynecol*. 2005;193:1630-9.
12. Skates SJ, Menon U, MacDonald N, *et al*. Calculation of the risk of ovarian cancer from serial CA-125 values for preclinical detection in postmenopausal women. *J Clin Oncol*. 2003;21 Suppl 10:206-10s.
13. Menon U, Skates SJ, Lewis S, *et al*. Prospective study using the risk of ovarian cancer algorithm to screen for ovarian cancer. *J Clin Oncol*. 2005;23:7919-26.
14. Berven FS, Flikka K, Berle M, *et al*. Proteomic-based biomarker discovery with emphasis on cerebrospinal fluid and multiple sclerosis. *Curr Pharm Biotechnol*. 2006;7:147-58.
15. Farina A, Dumonceau JM, Lescuyer P. Proteomic analysis of human bile and potential applications for cancer diagnosis. *Expert Rev Proteomics*. 2009;6:285-301.
16. Jamaspishvili T, Kral M, Khomeriki I, *et al*. Urine markers in monitoring for prostate cancer. *Prostate Cancer Prostatic Dis*. 2010;13:12-9.
17. Drake RR, White KY, Fuller TW, Igwe E, Clements MA, Nyalwidhe JO, *et al*. Clinical collection and protein properties of expressed prostatic secretions as a source for biomarkers of prostatic disease. *J Proteomics*. 2009;72:907-17.
18. Issaq HJ, Xiao Z, Veenstra TD. Serum and plasma proteomics. *Chem Rev*. 2007;107:3601-20. doi:10.1021/cr068287r.
19. Zhou M, Lucas DA, Chan KC, Issaq HJ, Petricoin 3rd EF, Liotta LA, *et al*. An investigation into the human serum "interactome". *Electrophoresis*. 2004;25:1289-98.
20. Wang YY, Cheng P, Chan DW. A simple affinity spin tube filter method for removing high-abundant common proteins or enriching low-abundant biomarkers for serum proteomic analysis. *Proteomics*. 2003;3:243-8.
21. Gundry RL, Van Eyk JE. Unraveling the complexity of circulating forms of brain natriuretic peptide. *Clin Chem*. 2007;53:1181-2.

22. Lowenthal MS, Mehta AI, Frogale K, Bandle RW, Araujo RP, Hood BL, *et al.* Analysis of albumin-associated peptides and proteins from ovarian cancer patients. *Clin Chem.* 2005;51:1933–45.
23. Tirumalai RS, Chan KC, Prieto DA, Issaq HJ, Conrads TP, Veenstra TD. Characterization of the low molecular weight human serum proteome. *Mol Cell Proteomics.* 2003;2:1096–103.
24. Liotta LA, Ferrari M, Petricoin E. Clinical proteomics: written in blood. *Nature.* 2003;425:905.
25. Rai AJ, Gelfand CA, Haywood BC, Warunek DJ, Yi J, Schuchard MD, *et al.* HUPO Plasma Proteome Project specimen collection and handling: towards the standardization of parameters for plasma proteome samples. *Proteomics.* 2005;5:3262–77.
26. Luchini A, Geho DH, Bishop B, *et al.* Smart hydrogel particles: biomarker harvesting: one-step affinity purification, size exclusion, and protection against degradation. *Nano Lett.* 2008;8:350–61.
27. Fredolini C, Meani F, Alex Reeder K, *et al.* Concentration and preservation of very low abundance biomarkers in urine, such as human growth hormone (hGH), by Cibacron Blue F3G-A loaded hydrogel particles. *Nano Res.* 2008;1:502–18.
28. Longo C, Patanarut A, George T, Bishop B, Zhou W, Fredolini C, *et al.* Core-shell hydrogel particles harvest, concentrate and preserve labile low abundance biomarkers. *PLoS One.* 2009;4(3):e4763 (Epub 2009 Mar 10.B).
29. Ahmed FE. Sample preparation and fractionation for proteome analysis and cancer biomarker discovery by mass spectrometry. *J Sep Sci.* 2009;32:771–9.
30. Mueller LN, Brusniak MY, Mani DR, Aebersold R. An assessment of software solutions for the analysis of mass spectrometry based quantitative proteomics data. *J Proteome Res.* 2008;7:51–61.
31. Streuli CH. Integrins and cell-fate determination. *J Cell Sci.* 2009;122:171–7.
32. Eliceiri BP. Integrin and growth factor receptor crosstalk. *Circ Res.* 2001;89:1104–10.
33. Danen EH, Yamada KM. Fibronectin, integrins, and growth control. *J Cell Physiol.* 2001;189:1–13.
34. Howe A, Aplin AE, Alahari SK, Juliano RL. Integrin signaling and cell growth control. *Curr Opin Cell Biol.* 1998;10:220–31.
35. Hall A. The cytoskeleton and cancer. *Cancer Metastasis Rev.* 2009;28:5–14.
36. Desgrosellier JS, Cheresch DA. Integrins in cancer: biological implications and therapeutic opportunities. *Nat Rev Cancer.* 2010;10:9–22.
37. Goel HL, Li J, Kogan S, Languino LR. Integrins in prostate cancer progression. *Endocr Relat Cancer.* 2008;15:657–64 (Epub 4 Jun 2008).
38. Monniaux D, Huet-Calderwood C, Le Bellego F, Fabre S, Monget P, Calderwood DA. Integrins in the ovary. *Semin Reprod Med.* 2006;24:251–61.
39. Mizejewski GJ. Role of integrins in cancer: survey of expression patterns. *Proc Soc Exp Biol Med.* 1999;222:124–38.
40. Weivoda S, Andersen JD, Skogen A, Schlievert PM, Fontana D, Schacker T, *et al.* ELISA for human serum leucine-rich alpha-2-glycoprotein-1 employing cytochrome c as the capturing ligand. *J Immunol Methods.* 2008;336:22–9 (Epub 4 Apr 2008).
41. Shirai R, Hirano F, Ohkura N, Ikeda K, Inoue S. Up-regulation of the expression of leucine-rich alpha(2)-glycoprotein in hepatocytes by the mediators of acute-phase response. *Biochem Biophys Res Commun.* 2009;382:776–9 (Epub 24 Mar 2009).
42. Andersen JD, Boylan KL, Xue FS, Anderson LB, Witthuhn BA, Markowski TW, *et al.* Identification of candidate biomarkers in ovarian cancer serum by depletion of highly abundant proteins and differential in-gel electrophoresis. *Electrophoresis.* 2010;31:599–610.
43. Kakisaka T, Kondo T, Okano T, Fujii K, Honda K, Endo M, *et al.* Plasma proteomics of pancreatic cancer patients by multi-dimensional liquid chromatography and two-dimensional difference gel electrophoresis (2D-DIGE): up-regulation of leucine-rich alpha-2-glycoprotein in pancreatic cancer. *Journal of Chromatography B: Analytical Technologies in the Biomedical and Life Sciences.* 2007;852:257–67.
44. Kawakami T, Hoshida Y, Kanai F, Tanaka Y, Tateishi K, Ikenoue T, *et al.* Proteomic analysis of sera from hepatocellular carcinoma patients after radiofrequency ablation treatment. *Proteomics.* 2005;5:4287–95.
45. Okano T, Kondo T, Kakisaka T, Fujii K, Yamada M, Kato H, *et al.* Plasma proteomics of lung cancer by a linkage of multi-dimensional liquid chromatography and two-dimensional difference gel electrophoresis. *Proteomics.* 2006;6:3938–48.
46. Chen Y, Lim BK, Hashim OH. Different altered stage correlative expression of high abundance acute-phase proteins in sera of patients with epithelial ovarian carcinoma. *J Hematol Oncol.* 2009;2:37.
47. Chen Y, Lim BK, Peh SC, Abdul-Rahman PS, Hashim OH. Profiling of serum and tissue high abundance acute-phase proteins of patients with epithelial and germ line ovarian carcinoma. *Proteome Sci.* 2008;6:20.
48. Weivoda S, Andersen JD, Skogen A, Schlievert PM, Fontana D, *et al.* ELISA for human serum leucine-rich alpha-2-glycoprotein-1 employing cytochrome c as the capturing ligand. *J Immunol Methods.* 2008;336:22–9. Epub 2008 Apr 4.
49. Schwartz DR, Kardia SL, Shedden KA, Kuick R, Michailidis G, Taylor JM, *et al.* Gene expression in ovarian cancer reflects both morphology and biological behavior, distinguishing clear cell from other poor-prognosis ovarian carcinomas. *Cancer Res.* 2002;62:4722–9.
50. Paschos KA, Canovas D, Bird NC. The role of cell adhesion molecules in the progression of colorectal cancer and the development of liver metastasis. *Cell Signal.* 2009;21:665–74 (Epub 7 Jan 2009).
51. Heyman L, Leroy-Dudal J, Fernandes J, Seyer D, Dutoit S, Carreiras F. Mesothelial vitronectin stimulates migration of ovarian cancer cells. *Cell Biol Int.* 2010;34:493–502.
52. Goodwin M, Yap AS. Classical cadherin adhesion molecules: coordinating cell adhesion, signaling and the cytoskeleton. *J Mol Histol.* 2004;35:839–44.
53. Felding-Habermann B, Cheresch DA. Vitronectin and its receptors. *Curr Opin Cell Biol.* 1993;5:864–8.
54. De Wever O, Derycke L, Hendrix A, De Meerleer G, Godeau F, Depypere H, *et al.* Soluble cadherins as cancer biomarkers. *Clin Exp Metastasis.* 2007;24:685–97.
55. Hurt EM, Chan K, Serrat MA, Thomas SB, Veenstra TD, Farrar WL. Identification of vitronectin as an extrinsic inducer of cancer stem cell differentiation and tumor formation. *Stem Cells.* 2010;28:390–8.
56. Cooper CR, Chay CH, Pienta KJ. The role of alpha(v)beta(3) in prostate cancer progression. *Cooper Neoplasia.* 2002;4:191–4.
57. Kuefer R, Hofer MD, Gschwend JE, *et al.* The role of an 80 kDa fragment of E-cadherin in the metastatic progression of prostate cancer. *Clin Cancer Res.* 2003;9:6447–52.
58. Kuefer R, Hofer MD, Zorn CS, Engel O, Volkmer BG, Juarez-Brito MA, *et al.* Assessment of a fragment of e-cadherin as a serum biomarker with predictive value for prostate cancer. *Br J Cancer.* 2005;92:2018–23.